

# Neurocomputing approach for the prediction of $\text{NO}_x$ emissions from CFBC in air-fired and oxygen-enriched atmospheres

Jarosław Krzywański<sup>a,\*</sup>, Wojciech Nowak<sup>b</sup>

<sup>a</sup>Jan Długosz University in Częstochowa, 13/15 Armii Krajowej Av., 42-200 Częstochowa, Poland;

<sup>b</sup>AGH University of Science and Technology, 30 Mickiewicza Av., 30-054 Krakow, Poland

## Abstract

This paper presents a way of predicting  $\text{NO}_x$  emissions from circulating fluidized bed combustors (CFBC) in air-fired and oxy-fuel conditions, using the Artificial Neural Network (ANN) Approach. The Original Neural Networks Model was successfully applied to calculate the  $\text{NO}_x$  (i.e.  $\text{NO} + \text{NO}_2$ ) emissions from coal combustion under air-fired and oxygen-enriched conditions in several CFB boilers. The ANN model was shown to give quick and accurate results in response to the input pattern. The  $\text{NO}_x$  emissions, evaluated using the developed ANN model are in good agreement with the experimental results.

**Keywords:** Nitrogen oxides; Circulating fluidized bed; Oxy combustion; Artificial neural networks

## 1. Introduction

Nitrogen oxides ( $\text{NO}_x$ ) are major gaseous pollutants CFB fossil fuel combustion, having injurious effects on the environment and human health [1]. The concentration of  $\text{NO}_x$  in flue gas is the result of competing formation and destruction mechanisms and is affected by complex factors. Among them are: fuel properties (particle size distribution, nitrogen and volatile content), excess oxygen, primary/secondary gas ratio, local temperature and oxygen partial pressure in the furnace, the presence of calcined limestone in the combustion chamber, gas velocity in the furnace, and the geometry of the system, as boiler size and exit effects influence the mixing processes and distribution of solids in the combustion chamber [2–31]. The height of the pilot-scale facilities used is smaller than the height of large-scale combustors, leading to a lowering of the gas residence time. Radial mixing of the fuel and of the secondary gas in the test facilities is more enhanced than it is in large-scale combustors [18]. For the oxy-fuel conditions the flue gas-recycle ratio should also be taken into account, considering the  $\text{NO}_x$  formation and destruction mechanisms, as part of the flue gas is recycled to the combustion chamber to control the combustion temperature [19, 21]. To obtain  $\text{NO}_x$  concentrations in flue gas, detailed measurements are generally needed, which are usually time consuming and expensive [2–4, 6–22, 26–35]. Other ways to evaluate the gaseous pollutants

emissions involve the use of several CFBC models. They differ as to their details and/or sophistication [5, 12, 25, 36–55]. Some of them refer to oxy-fuel conditions. Basu provided a wide-range review and comparison of circulating fluidized bed combustor models [5]. The author discussed two programming approaches to performance modeling, i.e., the furnace approach and the system approach. The furnace approach describes the details of what goes on in the furnace while the system approach focuses on system integration. In the furnace approach, models can be grouped under three levels of details and/or sophistication: level I: 1-D, plug flow/stirred tank, using simple mass and energy balance; level II: core-annulus, 1.5-D with broad consideration of combustion and other related processes; level III: 3-D model based on Navier-Stokes Equation with detailed consideration of chemical kinetics and individual physical processes. Gungor and Eskin [12] also underlined that all CFB models can be classified into three groups, according to the Harris and Davidson classification [36]. Models of Type I constitute the simple axial solids distribution models, Type II are core/annulus models and Type III—Computational Fluid Dynamics (CFD) models, which are the most general and numerically complex. The CFD models employ gas and solids continuity equations, momentum balances and constitutive equations [12]. As an example, Leckner and Lyngfelt [21] developed a two-dimensional coal combustion model in a CFB boiler. It was successfully validated against data from a pilot-scale 50 kW CFB combustor as well as an industrial scale 160 MW CFB boiler. A review of macroscopic (semi-empirical) models for fluid dynamics of circulating fluidized

\*Corresponding author

Email addresses: jkrzywanski@tlen.pl (Jarosław Krzywański),  
wnowak@agh.edu.pl (Wojciech Nowak)

bed boilers was also given by Pallares and Johnsson [55]. As the nature of the industrial processes is often non-linear and extremely complex, models usually include some empirical parameters to provide necessary data in the cases where up-to-date modeling is unsatisfactory [55]. It happens, e.g., to adjust parameters of the model, which could not be determined immediately, especially for different operating conditions. Models are often time consuming. The time required to acquire accurate predictions through numerical testing can be fairly long, in spite of the fact that they usually use simplified assumptions to make the models simpler and easier and to obtain a tractable solution. The algorithms are complicated and, as usual, are based on the solution of complex differential equations. Another estimation method in engineering analysis and predictions is applying techniques provided by artificial intelligence [43]. One of them is Artificial Neural Networks (ANNs). Compared to the complex numerical and analytical methods as well as the high costs of empirical experiments, neural networks constitute an alternative approach to data handling [56]. This paper presents ANN techniques to predict the  $\text{NO}_x$  (i.e.,  $\text{NO} + \text{NO}_2$ ) emissions from coal combustion under air-fired and oxygen-enriched conditions in CFB combustors. Simulation results agree well with experimental data, not only qualitatively. Moreover, the proposed methodology delivers quantitative agreement of calculated data with experimental results.

## 2. $\text{NO}_x$ emissions: theory

Many works deal with the  $\text{NO}_x$  emissions from CFB fossil fuel combustion, since nitrogen oxides are some of the most harmful components of flue gas from CFB boilers. Some of them are described in this section. Interesting studies of  $\text{NO}_x$  formation are presented by Zhao et al. [31]. The authors used a pilot CFB combustor with a riser which is 0.152 m square and 7.3 m tall. Five fuels were burned, i.e. (in order of decreasing rank) coals: anthracite, Minto (a high sulfur bituminous coal), Highvale (a subbituminous coal), lignite and petroleum coke. The authors underlined that oxidation of volatiles and char-bound nitrogen take part in  $\text{NO}_x$  formation. The local temperature, oxygen partial pressure and the presence of catalysts are also important factors as they have an impact on volatiles release and combustion processes. Reduction of  $\text{NO}_x$  is favored by the presence of char and the lower oxygen partial pressures, whereas the  $\text{NO}_x$  formation mechanism dominates for higher oxygen partial pressures and higher volatile release. The complex effect of the addition of limestone on  $\text{NO}_x$  formation was also observed. Generally, limestone is considered to be a factor leading to an increase in  $\text{NO}_x$  formation. The reason is that for high-volatile fuels (e.g. Minto coal —33.1% of volatile matter) calcined limestone surface acts as a catalyst for oxidation of volatile nitrogen. On the other hand, when the volatile content in fuel is low (e.g. 10% for petroleum coke) the presence of calcined limestone acts as a catalyst for NO reduction by CO and this mechanism becomes dominant in

such cases [31]. These results are consistent with the opinion that low rank coals can yield more  $\text{NO}_x$  than higher rank ones [13]. Luis et al. [8] used a CFB combustor with a riser of 0.161 m i.d. and 6.2 m high to investigate the influence of five operating parameters on  $\text{NO}_x$  emissions. Downmill bituminous coal was burned during the study. The effects of bed temperature, air staging, excess air, limestone addition and coal particle size were investigated in the study. The  $\text{NO}_x$  emission increased with the bed temperature due to the decrease in char and CO concentration. Higher temperatures also promoted the oxidation of NCO to NO. The  $\text{NO}_x$  emission increased with the excess air. Similar to the opinion expressed by Gungor and Eskin [12] the authors observed that higher oxygen concentration in the riser enhances the combustion of char and volatile matter especially in the lower part of the furnace and leads to an increase in  $\text{NO}_x$  formation. The char and CO concentration throughout the riser are also lower, which deteriorates the  $\text{NO}_x$  reduction mechanisms. The authors also confirmed that staged combustion is a useful method to decrease  $\text{NO}_x$  emission. The concentration of  $\text{NO}_x$  in flue gas decreased as the secondary air ratio increases. The authors give three reasons for this. First of all, atmosphere with limited oxygen in the lower zone of the combustion chamber tends to conversion of volatiles-N to  $\text{N}_2$  instead of  $\text{NO}_x$ . A higher secondary air ratio also leads to an increase in char and CO concentration in the lower part of the furnace, causing higher NO decomposition. Finally the residence time of gas in the bottom zone of the combustion chamber increases with the secondary air ratio. As a result, the  $\text{NO}_x$  decomposition becomes a more dominant mechanism over  $\text{NO}_x$  formation, throughout the height of the combustion chamber. The coal particle size slightly influences the  $\text{NO}_x$  emission [8], which increases with a mean coal particle diameter. One of the explanation is based on the difference between the intensity of combustion and devolatilization processes for fine and coarse particles. The complex dependence of  $\text{NO}_x$  emission on CaO addition has been also discussed by Luis et al. [8]. The decrease in NO emission with  $\text{SO}_2$  was explained by the CO oxidation inhibition that occurs in the presence of sulfur dioxides. The  $\text{NO}_x$  emission increased with the Ca/S molar ratio, due to the catalytic effect of CaO. The authors also observed the reverse mechanism, when limestone addition leads an NO decrease because CaO acts as the catalyst for NO reduction. Such effects are responsible for differences in  $\text{NO}_x$  emissions reported by Amand et al. [2] and the results agree with the data shown in [31, 32]. The influence of limestone addition at two different positions in the riser on gaseous pollutants emissions were investigated during the study. Limestone was injected at the bottom of the riser and above the secondary air injection of a CFB system. The influence of this undertaking was small and resulted in the difference of about 10 ppm in NO/  $\text{NO}_x$  emissions. One of the reasons is the long volatile-N time release, according to the observations reported by Zhao et al. [31]. The dependence between  $\text{NO}_x$  emissions and the Ca/S ratio was also observed by Feng et al. [10]. During combustion of coal containing 20.9% of volatile mat-

ter in CFB combustor the  $\text{NO}_x$  concentrations increased with the Ca/S ratio. It seems that to attain the volatile content of 20.9% calcined limestone surface still acts as a catalyst for volatile nitrogen oxidation [31]. The scale-up problem of CFB boilers with respect to pollutants emissions was investigated by Knobig et al. [18]. Industrial-size 12 MWth CFB combustor (height: 14 m, cross-sectional area of the riser: 1.6 m x 1.6 m) and lab-scale facility (height: 16 m, inner diameter of the riser: 0.1 m) were used during the study. Although the axial NO concentration profiles of both combustors had basically the same shape, the general finding was that some significant deviations of the profiles can be also recognized. The authors pointed out three-dimensional effects in the large-scale combustor as well as differences in particle size distribution in the fuel feed [18]. The importance of air staging in NO emissions was also described in [19–21]. The authors observed that advanced air staging, when the second stage is located after the separation of the solid particles from the flue gas, leads to a significant reduction in NO. The results obtained by Amand and Leckner [3] revealed that NO emissions depend on the char loading of the boiler and the existence of unburned combustible matter such as CO and  $\text{H}_2$  in the gas phase, whereas these parameters are influenced also by the bed temperature, fuel type and the air-to-fuel ratio in the furnace. The authors also confirmed that the NO emissions tend to increase with the volatiles content in the fuel used in the study [4].  $\text{NO}_x$  emissions under different operating conditions were also investigated by Gungor [11]. The experiments were carried out on 50 kW and 80 kW pilot-scale CFB combustors as well as a 160 MW large-scale CFB boiler. The author observed that  $\text{NO}_x$  emissions decreased with the air excess and inlet bed pressure, and increased with the operational bed velocity. The effect of the ash recirculating ratio on  $\text{NO}_x$  emissions from a CFB combustor was studied by Feng et al. [10]. The  $\text{NO}_x$  concentration in flue gas decreased with ash recirculation ratio. There are also some results concerning  $\text{NO}_x$  emissions from CFB boilers operated under oxygen-enriched atmospheres [6, 7, 9, 14, 17–26, 30–57]. The Mini-CFBC 75 kW<sub>th</sub> boiler with a riser of 0.1 m i.d. and 5 m tall was used to study oxy-fuel combustion with flue gas recycle [17]. Bituminous and sub-bituminous coals were fired. An increase in  $\text{NO}_x$  concentration in flue gas was reported during the oxy-fuel combustion. In spite of the fact that the  $\text{NO}_x$  concentration was twice as high as under the air-firing mode, the total amount of  $\text{NO}_x$  emitted was about the same due to the lower flue gas volume from the oxy-fuel-fired unit. Similar results were obtained by Canmet ENERGY [14–16, 28], Nsakala et al. [26] and Varonen et al. [30]. Slightly different results are presented in [9]. A pilot-scale (30–100 kW) CFB reactor was used to carry out a set of tests performed under oxy-fired conditions at VTT Finland. The NO emissions were comparable with those obtained during air mode. The above literature review indicates the complexity of the  $\text{NO}_x$  emissions mechanism occurring during coal combustion, both in air-fired and oxy-fuel CFB conditions. As the discussion about dominant mechanisms over the  $\text{NO}_x$  formation is still open,

especially in oxy-fuel conditions, there is a clear need for a simple to use and reliable model that can quickly and accurately predict  $\text{NO}_x$  emissions from different combustors over a range of unit dimensions, operating conditions and physical properties of fuel burned in the CFB boilers. In this paper the authors present a model of  $\text{NO}_x$  emissions developed using the artificial neural network approach. The necessary data for this work to train the neural network was collected from experiments presented in the literature. The data set consisted of 70 patterns including experimental results from large- and pilot-scale CFB combustors, operated both under air-fired and oxygen-enriched conditions.

### 3. Results and discussion

#### 3.1. Neural network modeling

Artificial neural networks (ANN) are useful in many fields of science, knowledge and technology. They provide an alternative approach to the simulation of complex, ill-defined and uncertain systems [55, 57–59]. Among others ANN are used in atmospheric sciences and energy engineering systems. Kalogirou [56] divided all the ANN applications into the following groups: classification, forecasting, control systems, optimization and decision-making. Giving some examples the author listed among others: modeling of the combustion processes in incineration plants, the predictive control of a thermal plant, modeling of the chemical reactions in turbulent combustion simulations [60–62]. Other examples of ANN applications include: modeling of engine emissions, control and modeling of power generation systems, load forecasting and prediction, chemical reactor modeling, air-quality prediction, heat transfer analysis, robotics [23, 24, 52, 58–86]. Liukkonen et al. [23, 24] used an unsupervised artificial neural network, Kohonen self-organizing map and multilayer perceptrons for the prediction of  $\text{NO}_x$  emissions from utility-scale atmospheric CFB boilers. An ANN model was applied to predict the  $\text{NO}_x$  emissions from a 600 MW capacity pulverized coal combustion boiler [65, 86]. Jensen et al. [58] implemented the neural network to investigate mercury speciation emissions from coal fired boilers. A special issue of Chemical Engineering and Processing was dedicated to the application of neural network, soft and hybrid computing in the area of multiphase reactors [87]. Some papers deal with the application of neural networks in the area of hydrodynamics and mass transfer [88–90], reactor design and scale up with the presence of chemical reactions [90–93]. Neural networks enjoy popularity because of their features. As they can learn the relationship between the input and output variables from given examples, they do not need any detailed information about the studied processes, unlike multiple linear and non-linear regression [56]. They operate like a “black box” and their learning process resembles the operation of a human brain [58, 63]. They have the ability to ignore redundant and excess data, use incomplete data sets and concentrate on more important inputs [56, 58, 59]. Since a single

neuron has a limited memorizing capacity, a neural network consists of a group of interconnected (by so-called weights) neurons (perceptrons) [58, 63]. The knowledge about the process acquired by the model during the learning stage is stored in the ANN structure and weights [56, 84]. The studied process involves the ANN's architecture, the activation function of a neurons and the number of perceptrons. Therefore there are, e.g., recurrent, feed-forward, Kohonen, Hopfield, probabilistic and Bayesian–Gaussian neural networks [23, 24, 58, 72, 90, 94]. Some of them refer to supervised, others to unsupervised or self-organizing neural networks. In this paper a multilayer ANN was applied since feed-forward neural networks are widely used in engineering applications [56, 58, 63, 82]. Perceptrons in such networks are arranged in three kinds of layers and form input, intermediate (so-called hidden) and output layers. Such ANNs can contain one or more hidden layers. Suitable architecture and the appropriate number of hidden neurons must be established for the ANN model, to achieve the required accuracy of neural network estimation. Therefore, in order to constitute a useful tool, a neural network needs to be prepared in advance in the following principle steps: setting ANN architecture initial values of weights (between 0 and 1), normalization of input and output signals, training (learning) process [59, 71]. The learning stage applied in this study consists of supervised learning, where the input pattern is repeatedly and simultaneously presented with its corresponding output pattern. For example, during overall heat transfer calculations such data sets consisted of 64, 29 and 69 input and output patterns, for membrane-walls, SH I and SH II, respectively [72]. The learning process allows one to modify the connection weights through a suitable learning method and to adjust them to produce the desired output. The ability of the artificial neural network to reproduce a process from training examples is called the neurocomputing approach and differs from programmed computing approach, which consists of writing algorithms using a mathematical model of the studied process [58]. A simple, powerful and reliable training method, often used to train artificial feed-forward neural networks, is the Back Propagation (BP) scheme [56, 69]. The BP technique is an iterative gradient algorithm for minimization of the mean square error between the desired and predicted output. In the BP scheme the difference between outputs and the pattern is the measure of the weights modification rate. The logarithmic sigmoid and the hyperbolic tangent sigmoid function are the most commonly used activation functions in such neural networks. Different activation functions can also be applied in each layer of the network [63]. When the criterion of the mean square error is fulfilled and the network has good generalization ability (i.e., the ability to accurately predict the validation data set, not previously seen in the neural network) the learning step is finished [63]. A neural network prepared in this way is a useful tool for performing quick, non-iterative calculations [58].

### 3.2. Model evaluation for NO<sub>x</sub> emission in air-fired and oxygen-enriched CFB conditions

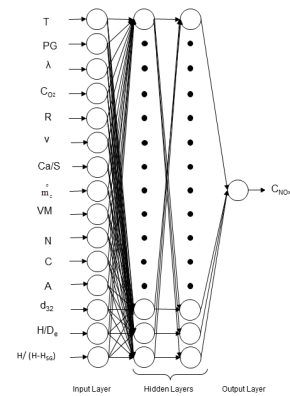


Figure 1: The structure of the multilayer neural network

The idea of using ANN previously emerged for the prediction of the overall heat transfer coefficient for membrane walls, Superheater I (SH I, Omega Superheater) and Superheater II (SH II, Wing-Walls) in the combustion chamber of the large-scale 260 MW<sub>e</sub> CFB boiler [72]. A similar approach was taken in this paper to create a simple and reliable model for the estimation of NO<sub>x</sub> concentration in flue gas during coal combustion in large- and small-scale CFB boilers operating in air-fired and oxygen-enriched conditions. The architecture of the neural network applied in the paper is shown in Fig. 1. The neural network is made of four layers: the input layer, two hidden layers and the output layer.

Table 1: Input parameters used for training and testing ANN

Input parameter	Range of values
Operating Conditions	
T, K	990 – 1251
PG, -	0.40 – 1.0
$\lambda$ , -	1.10 – 2.23
CO <sub>2</sub> , -	0.209 – 0.450
R, -	0.0 – 0.702
v, m/s	1.75 – 8.30
Ca/S, -	0.0 – 6.7
m <sub>C</sub> , kg/s	0.000972 – 61.6
Fuel properties (Air-Dried Basis)	
VM, wt. %	11.0 – 37.9
A, wt. %	1.0 – 38.3
C, wt. %	26.8 – 86.9
N, wt. %	0.34 – 2.1
d <sub>32</sub> , m	0.00004 – 0.006
Geometry parameters	
H/D <sub>e</sub> , -	3.04 – 50.0
H/(H-H <sub>SG</sub> ), -	1.0 – 1.4

The number of neurons in the input and output layers are the same as the number of input and output parameters, respectively. A highly accurate model for the prediction of NO<sub>x</sub> emissions needs some detailed information of CFB combustors, as they are different in size, they have different height and cross-section of the combustion chamber, e.g. circular, square and rectangular, some of them are large- whilst others small-scale boilers [8, 11, 12, 15–17, 22, 95, 96]. Most of

them have been fitted with cyclones, but the 261 MW<sub>e</sub> COM-PACT CFB boiler operated in Turów Power Station in Poland is equipped with two compact separators, providing an example of second generation boiler design [46, 95, 96]. The fuel properties and operating parameters for both air-fired and oxygen-enriched conditions should be taken into account for the purposes of accurately training the ANN model. An attempt has been made to apply all possible factors that affect NO<sub>x</sub> emissions. Therefore the set of input parameters consists of a number of operating conditions, fuel properties and geometry factors of the combustion chamber. The input parameters are as follows: the average bed temperature  $T$ , the primary gas ratio  $PG$ , the excess oxygen  $\lambda$ , the oxygen concentration in the inlet gas  $C_{O_2}$ , the flue gas recycle ratio  $R$ , the average gas velocity in the riser  $v$ , the Ca/S molar ratio, coal feed rate, volatile matter VM, nitrogen N, carbon C and ash A content in the coal, the Sauter mean diameter of the coal particles  $d_{3,2}$  and two geometry factors:  $H/D_e$ ,  $H/(H - H_{SG})$ . The R parameter is the ratio of recycled flue gas to the total amount of flue gas from coal combustion. For the cases when the boiler was not supplied by secondary gas the parameter  $H_{SG}$  is assumed to be 0 for calculation purposes. The input parameters and their ranges are given in Table 1. The carbon and ash content in the fuel as well as the coal feed rate are taken into account by the model among the input parameters, as they can be easily acquired from fuel analysis and operating conditions. These parameters also improve the accuracy of the model and have been shown to be important for NO<sub>x</sub> emissions [23, 24]. For example, the fuel feed rate is directly connected with the load of the boiler, thereby influencing the NO<sub>x</sub> emissions. The output variable is the NO<sub>x</sub> concentration in flue gas. For the assumed data set the output and input layers consist of one and fifteen neurons, respectively. One Back Propagation scheme called the Lee and Park's algorithm, consisting in simultaneous changing the momentum and learning rate during the training phase, was applied for normalization of input and output parameters [71]. The coefficient of determination  $R^2$  of the linear regression line between the predicted values from the neural network and the desired output, the mean absolute error MAE and the mean relative error MRE were used in order to select the optimal number of neurons in the hidden layers.

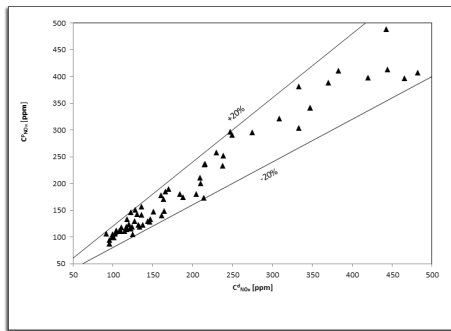
On the basis of the preliminary calculations as well as previous experience [71], the hyperbolic tangent sigmoid function is applied as the activation function for all perceptrons. ANN models with the hyperbolic tangent sigmoid function produce higher coefficients of determination and lower errors compared to ANN models with the logarithmic sigmoid activation function. The inputs consisted of 70 input-output data sets, obtained from large- and small-scale, atmospheric CFB boilers, operating under air-fired and oxygen-enriched modes, reported in the literature [7, 8, 11, 12, 15–17, 22, 37, 95]. The simulations are carried out for air-firing as well as three different oxygen-enriched conditions, i.e., when combustion runs in a gas mixture based on O<sub>2</sub> and N<sub>2</sub>, and also when combustion takes place in N<sub>2</sub>-free atmo-

Table 2: Errors of the NO<sub>x</sub> emissions for different ANNs

Model	Structure	R <sup>2</sup>	MAE	MRE
1	15-3-3-1	0.9044	25.875	0.141
2	15-3-6-1	0.9352	18.992	0.087
3	15-3-9-1	0.9303	19.254	0.089
4	15-3-12-1	0.9431	18.295	0.084
5	15-3-15-1	0.9399	18.931	0.090
6	15-6-3-1	0.9264	19.776	0.090
7	15-6-6-1	0.9236	20.667	0.097
8	15-6-9-1	0.9347	19.145	0.088
9	15-6-12-1	0.9375	18.590	0.085
10	15-6-15-1	0.9332	18.760	0.085
11	15-9-3-1	0.9066	24.302	0.123
12	15-9-6-1	0.9334	18.883	0.087
13	15-9-9-1	0.9332	19.06	0.088
14	15-9-12-1	0.9476	17.253	0.080
15	15-9-15-1	0.9317	19.958	0.093
16	15-12-3-1	0.9140	21.848	0.103
17	15-12-6-1	0.9213	20.954	0.101
18	15-12-9-1	0.9254	19.576	0.091
19	15-12-12-1	0.9160	20.889	0.097
20	15-12-15-1	0.9324	19.761	0.094
21	15-15-3-1	0.9251	20.694	0.104
22	15-15-6-1	0.9112	24.913	0.138
23	15-15-9-1	0.9214	19.797	0.089
24	15-15-12-1	0.9248	19.268	0.087
25	15-15-15-1	0.9302	19.126	0.087

spheres of O<sub>2</sub>/CO<sub>2</sub> and O<sub>2</sub>/RFG (Recycled Flue Gas), with various fractions of oxygen. These data sets were applied for both training and testing of the developed ANN model. Since the performance of an ANN depends on its structure, different architectures were tested as the ability of the network to extract the knowledge of the studied process can be improved with new perceptrons. The number of hidden neurons varied from 1 to 15 in each hidden layer. This approach helped cut the risk of memorization instead of generalization of the relationship between input and output data [63, 78]. This procedure resulted in the need to study and analyze 225 different ANN architectures in total, with various numbers of hidden neurons. The selected ANNs with the number of hidden perceptrons increasing by every three neurons are given in Table 2. The optimal network was selected from 255 networks based on the above error measures. All the calculations were performed in the C++ programming language. 3.3. When selecting the optimal structure based on observations of the learning processes, a neural network with a higher number of hidden neurons generally produced smaller errors and needed fewer training epochs to obtain good results compared to ANN models with few hidden perceptrons. The training of neural networks containing more hidden neurons also proceeded more effectively and the mean square error decreased more quickly compared to the network containing fewer hidden neurons. The best ANN architecture turned out to be the [15-9-12-1] model, with the highest coefficient of determination  $R^2$  equal to 0.9476 as well as the lowest errors: mean absolute error (17.253) and mean relative error (0.08).

Another interesting ANN is the [15-3-12-1] architecture, but  $R^2$  is lower and error measures (MAE, MRE) are higher than with the [15-9-12-1] type ANN model. Therefore, the [15-9-12-1] ANN is the optimal configuration for the consid-



estimated by [15-9-12-1] type of ANN are shown in Fig. 2.

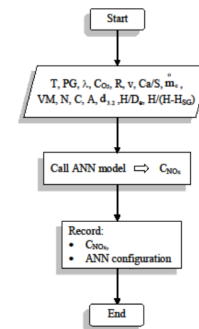


Figure 2: Comparison of NO<sub>x</sub> emissions desired and predicted by the [15-9-12-1] ANN model

Figure 3: Application of the ANN for calculating NO<sub>x</sub> emissions

Table 3: NO<sub>x</sub> emissions desired and predicted by the model

	$C_{NO_x}^d$ ppm	$C_{NO_x}^p$ ppm	$\delta$ %
Data used for training network	117.70	118.71	0.86
	347.80	341.64	1.77
	164.00	170.95	4.24
	138.14	122.52	11.30
	117.00	117.03	0.02
	443.00	487.86	10.13
oxy-fuel conditions	333.00	303.88	8.75
	210.00	200.59	4.48
	309.00	321.02	3.89
	215.00	235.83	9.69
	117.50	114.72	2.37
air-fired conditions	188.00	174.81	7.02
	132.34	122.49	7.45
	444.40	412.41	7.20
	99.10	99.49	0.40
Data not used for training network	250.00	290.77	16.31
	216.00	237.13	9.78
	579.00	464.75	19.73
	230.00	257.52	11.97
	238.00	233.29	1.98

Good accuracy in the prediction of NO<sub>x</sub> emissions from coal combustion in CFB boilers operated both in air-fired and oxy-fuel conditions was obtained.

The prepared ANN model is a tool capable of optimizing operating conditions in order to keep under control the NO<sub>x</sub> emissions from coal combustion in CFB boilers. The model can be easily applied to calculate NO<sub>x</sub> concentrations via the non-iterative procedure. The flow chart of such ANN application is given in Fig. 3.

ered task and this model is used for further calculations. The [15-9-12-1] type network consists of twenty one hidden neurons with nine and twelve perceptrons in the first and the second hidden layer, respectively. The ANN model was tested after the learning stage using samples, both training and new ones, unseen before in the network. Some of the results of NO<sub>x</sub> emissions, predicted by the [15-9-12-1] ANN model as well as desired values obtained from experiments are shown in Table 3. The NO<sub>x</sub> concentrations predicted by [15-9-12-1] ANN model are located within the limits of ±20% related to the experimental data. The relative errors  $\delta$  between and for most of the data given in Table 3, even for data previously unseen by the network (new data, not previously used for training) are less than 10% and in some cases—even less than 1%. The maximum and minimum values of the relative error are equal to 19.73% and 0.02%, respectively. The comparison between NO<sub>x</sub> emissions obtained from experiments for different operating conditions and the corresponding data

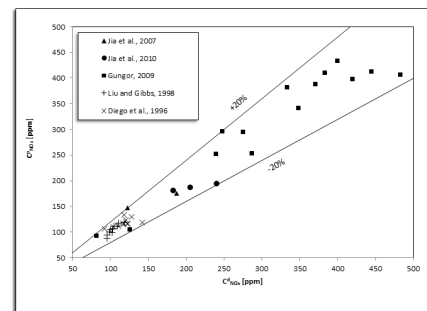


Figure 4: Comparison of the NO<sub>x</sub> emissions desired and predicted by [15-9-12-1] type ANN for air-fired CFB conditions

The results of the non-iterative neurocomputing calculations carried out for air-fired and oxygen-enriched conditions are given in Fig. 4 and Fig. 5, respectively.

The measured data of NO<sub>x</sub> emissions, corresponding to air-fired and oxy-fuel conditions, taken from literature [8, 11, 12, 15–17, 22] are regarded as the desired values.

The ANN model correctly predicts the NO<sub>x</sub> emissions from coal combustion in CFB boilers, both for air-fired and oxygen-enriched conditions, i.e., the ANN model predicts accurate results compared to experimental data.



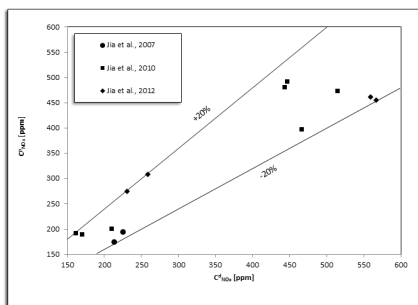


Figure 5: Comparison of the NO<sub>x</sub> emissions desired and predicted by [15-9-12-1] type ANN for oxy-fuel CFB conditions

#### 4. Conclusion

In this study the ANN model was developed to determine the NO<sub>x</sub> emission from coal combustion in the CFB boilers, in air-fired and oxygen-enriched conditions. The best feed-forward ANN topology was established, appropriate for the task considered in the paper, under a wide range of operating conditions. The model provides quick and reliable predictions of NO<sub>x</sub> emissions for both large- and small-scale CFB combustors for any input pattern of the boiler operating parameters (under different conditions). The model considers a wide range of parameters influencing NO<sub>x</sub> formation from coal combustion in CFB boilers. All results obtained using the ANN model are located within the limits of  $\pm 20\%$  compared to the experimental data, but some of them are even lower than 1%. The model with tangent sigmoid activation function is capable of predicting the NO<sub>x</sub> emission with good accuracy and can be applied to solve and generalize the complex relationship between NO<sub>x</sub> emissions and operational parameters for a variety of CFB boilers of different capacity. Taking into account these abilities, the ANN model constitutes a very effective tool for the purposes of simulation and optimization of CFB systems.

#### Acknowledgments

The financial support of this work by the Polish Government, as part of Framework Project: Supercritical Coal-fired Power Units, is gratefully acknowledged.

#### References

- [1] National Center for Environmental Assessment-RTP Division, Office of Research and Development, U.S. Environmental Protection Agency, Research Triangle Park, EPA/600/R-08/082F. Integrated Science Assessment for Oxides of Nitrogen - Health Criteria (2008).
- [2] L. Amand, B. Leckner, K. Dam-Johansen, Influence of SO<sub>2</sub> on the NO/N<sub>2</sub>O chemistry in fluidized bed combustion: 1. full-scale experiments, *Fuel* 72 (1993) 557–564.
- [3] L.-E. Åmand, B. Leckner, Influence of fuel on the emission of nitrogen oxides (NO and N<sub>2</sub>O) from an 8-MW fluidized bed boiler, *Combustion and Flame* 84 (1-2) (1991) 181–196.
- [4] L. Amand, B. Leckner, The role of fuel volatiles for the emission of nitrogen oxides from fluidized bed boilers - a comparison between designs, in: *Proc. of the 23rd International Symposium on Combustion*, 1990, pp. 927–933.
- [5] P. Basu, Combustion of coal in circulating fluidized-bed boilers: a review, *Chemical Engineering Science* 54 (22) (1999) 5547–5557.
- [6] E. Bool, S. Laux, E. Eddings, Oxy-coal combustion in small-scale CFB, in: *Proc. Of th 35th International Technical Conference on Clean Coal & Fuel Systems*, Florida, USA, 2010, pp. 190–196.
- [7] T. Czakiert, W. Muskala, S. Jankowska, G. Krawczyk, P. Borecki, L. Jesionowski, W. Nowak, The effect of oxygen concentration on nitrogen conversion in oxy-fuel CFB environment, in: *21 International Conference on fluidized bed combustion*, Naples, Italy, 2012, pp. 495–502.
- [8] F. Luis, C. A. Londono, X. S. Wang, B. M. Gibbs, Influence of operating parameters on nox and n<sub>2</sub>o axial profiles in a circulating fluidized bed combustor, *Fuel* 75 (8) (1996) 971–978.
- [9] T. Eriksson, O. Sippu, A. Hotta, M. K. Zhen Fan, T. Hyppänen, T. Pikkariainen, Oxyfuel CFB boiler as a route to near zero CO<sub>2</sub> emission coal firing, in: *Power-GEN Europe*, 2007, pp. 26–28.
- [10] B. Feng, H. Liu, J.-W. Yuan, Z.-J. Lin, D.-C. Liu, B. Leckner, Nitrogen oxides emission from a circulating fluidized bed combustor, *International Journal of Energy Research* 20 (11) (1996) 1015–1025.
- [11] A. Gungor, Prediction of so<sub>2</sub> and no<sub>x</sub> emissions for low-grade turkish lignites in cfb combustors, *Chemical Engineering Journal* 146 (3) (2009) 388–400.
- [12] A. Gungor, N. Eskin, Two-dimensional coal combustion modeling of cfb, *International Journal of Thermal Sciences* 47 (2) (2008) 157–174.
- [13] A. Hayhurst, A. Lawrence, The amounts of nox and n<sub>2</sub>o formed in a fluidized bed combustor during the burning of coal volatiles and also of char, *Combustion and flame* 105 (3) (1996) 341–357.
- [14] L. Jia, Y. Tan, D. McCalden, Y. Wu, I. He, R. Symonds, E. Anthony, Commissioning of a 0.8 mw th cfb for oxy-fuel combustion, *International Journal of Greenhouse Gas Control* 7 (2012) 240–243.
- [15] L. Jia, Y. Tan, Y. Wu, E. Anthony, Oxy-fuel combustion tests using a 0.8 mwth pilot-scale circulating fluidized bed, in: *Proceedings of the 21st International Conference on Fluidized Bed Combustion*, Naples, Italy, 2012, pp. 381–388.
- [16] L. Jia, Y. Tan, E. Anthony, Emissions of so<sub>2</sub> and no<sub>x</sub> during oxy-fuel cfb combustion tests in a mini-circulating fluidized bed combustion reactor, *Energy & Fuels* 24 (2) (2009) 910–915.
- [17] L. Jia, Y. Tan, C. Wang, E. Anthony, Experimental study of oxy-fuel combustion and sulfur capture in a mini-cfb, *Energy & Fuels* 21 (6) (2007) 3160–3164.
- [18] T. Knöbig, J. Werther, L.-E. Åmand, B. Leckner, Comparison of large- and small-scale circulating fluidized bed combustors with respect to pollutant formation and reduction for different fuels, *Fuel* 77 (14) (1998) 1635–1642.
- [19] B. Leckner, Fluidized bed combustion: mixing and pollutant limitation, *Progress in Energy and Combustion Science* 24 (1) (1998) 31–61.
- [20] B. Leckner, L.-E. Åmand, K. Lücke, J. Werther, Gaseous emissions from co-combustion of sewage sludge and coal/wood in a fluidized bed, *Fuel* 83 (4) (2004) 477–486.
- [21] B. Leckner, A. Lyngfelt, Optimization of emissions from fluidized bed combustion of coal, biofuel and waste, *International journal of energy research* 26 (13) (2002) 1191–1202.
- [22] H. Liu, B. M. Gibbs, The influence of limestone addition at different positions on gaseous emissions from a coal-fired circulating fluidized bed combustor, *Fuel* 77 (14) (1998) 1569–1577.
- [23] M. Liukkonen, M. Heikkinen, T. Hiltunen, E. Hälikkää, R. Kuivalainen, Y. Hiltunen, Artificial neural networks for analysis of process states in fluidized bed combustion, *Energy* 36 (1) (2011) 339–347.
- [24] M. Liukkonen, T. Hiltunen, E. Hälikkää, Y. Hiltunen, Modeling of the fluidized bed combustion process and no<sub>x</sub> emissions using self-organizing maps: an application to the diagnosis of process states, *Environmental Modelling & Software* 26 (5) (2011) 605–614.
- [25] D. Mao, J. R. Edwards, A. V. Kuznetsov, R. K. Srivastava, Three-dimensional numerical simulation of a circulating fluidized bed reactor for multi-pollutant control, *Chemical engineering science* 59 (20)

- (2004) 4279–4289.
- [26] N. Nsakala, G. Liljedahl, D. Turek, Greenhouse gas emissions control by oxygen firing in circulating fluidized bed boilers: Phase II – pilot scale testing and updated performance and economics for oxygen fired CFB, Tech. rep., PPL Report No. PPL-04-CT-25 under cooperative agreement No. DE-FC26-01NT41146 (2004).
- [27] G. Scheffknecht, L. Al-Makhadmeh, U. Schnell, J. Maier, Oxy-fuel coal combustion—a review of the current state-of-the-art, *International Journal of Greenhouse Gas Control* 5 (2011) S16–S35.
- [28] Y. Tan, L. Jia, Y. Wu, E. Anthony, Experiences and results on a 0.8 m<sup>2</sup> oxy-fuel operation pilot-scale circulating fluidized bed, *Applied Energy* 92 (2012) 343–347.
- [29] M. B. Toftegaard, J. Brix, P. A. Jensen, P. Glarborg, A. D. Jensen, Oxy-fuel combustion of solid fuels, *Progress in energy and combustion science* 36 (5) (2010) 581–625.
- [30] T. Klajny, J. Krzywanski, W. Nowak, Mechanism and kinetics of coal combustion in oxygen enhanced conditions, in: 6th International Symposium on Coal Combustion, Wuhan, China, 2007, pp. 148–153.
- [31] J. Zhao, C. Brereton, J. R. Grace, C. J. Lim, R. Legros, Gas concentration profiles and NO<sub>x</sub> formation in circulating fluidized bed combustion, *Fuel* 76 (9) (1997) 853–860.
- [32] L. Duan, C. Zhao, W. Zhou, C. Qu, X. Chen, O<sub>2</sub>/CO<sub>2</sub> coal combustion characteristics in a 50kw th circulating fluidized bed, *International Journal of Greenhouse Gas Control* 5 (4) (2011) 770–776.
- [33] T. Eriksson, K. Nuortimo, A. Hotta, K. Myöhänen, T. Hyppänen, T. Pikkarainen, Near zero CO<sub>2</sub> emissions in coal firing with oxyfuel cfb boiler, in: Proc. of the 9th International Conference on Circulating Fluidized Beds, Hamburg, Germany, May, 2008, pp. 13–16.
- [34] A. Blaszcuk, W. Nowak, S. Jagodzick, Effects of operating conditions on denox system efficiency in supercritical circulating fluidized bed boiler, *Journal of Power Technologies* 93 (1) (2013) 1.
- [35] A. Blaszcuk, M. Komorowski, W. Nowak, Distribution of solids concentration and temperature within combustion chamber of sc-otc cfb boiler, *Journal of Power Technologies* 92 (1) (2012) 27–33.
- [36] B. Harris, J. Davidson, Modelling options for circulating fluidized beds: a core/annulus deposition model, *Circulating fluidized bed technology IV* (1994) 32.
- [37] J. Krzywański, T. Czakiert, W. Muskała, W. Nowak, Modelling of CO<sub>2</sub>, CO, SO<sub>2</sub>, O<sub>2</sub> and NO<sub>x</sub> emissions from the oxy-fuel combustion in a circulating fluidized bed, *Fuel Processing Technology* 92 (3) (2011) 590–596.
- [38] J. Krzywanski, T. Czakiert, W. Muskała, R. Sekret, W. Nowak, Modeling of solid fuels combustion in oxygen-enriched atmosphere in circulating fluidized bed boiler: Part 1. The mathematical model of fuel combustion in oxygen-enriched CFB environment, *Fuel Processing Technology* 91 (3) (2010) 290–295.
- [39] J. Krzywanski, T. Czakiert, W. Muskała, R. Sekret, W. Nowak, Modeling of solid fuel combustion in oxygen-enriched atmosphere in circulating fluidized bed boiler: Part 2. Numerical simulations of heat transfer and gaseous pollutant emissions associated with coal combustion in O<sub>2</sub>/CO<sub>2</sub> and O<sub>2</sub>/N<sub>2</sub> atmospheres enriched with oxygen under circulating fluidized bed conditions, *Fuel Processing Technology* 91 (3) (2010) 364–368.
- [40] W. Muskała, J. Krzywiński, R. Sekret, W. Nowak, Model research of coal combustion in circulating fluidized bed boilers, *Chemical and Process Engineering* 29 (2008) 473–492.
- [41] K. Myöhänen, T. Hyppänen, M. Loschkin, Converting measurement data to process knowledge by using three-dimensional cfb furnace model, in: The 8th International Conference on CFB, 2005.
- [42] D. Pallares, F. Johnsson, M. Palonen, A comprehensive model of cfb combustion, in: 9th Int. Conf. on Circulating Fluidized Beds, 2008.
- [43] M. Palonen, D. Pallares, A. Larsson, F. Johnsson, V. Ylä-Outinen, J. Laine, Circulating fluidized bed combustion-build-up and validation of a three-dimensional model.
- [44] T. Pikkarainen, A. Tourunen, H. Nevalainen, T. Leino, J. Saastamoinen, T. Eriksson, Small scale fluidized bed experiments under oxygen combustion conditions, in: International Conference on Coal Science & Technology, University of Nottingham UK, 2007.
- [45] J. Saastamoinen, A. Tourunen, T. Pikkarainen, H. Häsä, J. Miettinen, T. Hyppänen, K. Myöhänen, Fluidized bed combustion in high concentrations of O<sub>2</sub> and CO<sub>2</sub>, in: 19th FBC Conference, 2006.
- [46] J. Werther, Fluid dynamics, temperature and concentration fields in large-scale cfb combustors, in: 8-th International Conference on Circulating Fluidized Beds, 2005.
- [47] N. Zhang, B. Lu, W. Wang, J. Li, 3D CFD simulation of combustion in a 150 MWe circulating fluidized bed boiler, in: Proc. of the 10-th International Conference on Circulating Fluidized Beds and Fluidization Technology - CFB-10, Sunriver, Oregon, USA, 2011, pp. 537–544.
- [48] C. Zhao, W. Zhou, L. Duan, X. Chan, 2d Euler-Euler simulation of oxy-coal combustion in a circulating fluidized bed., in: Proc. of the 21 International Conference on fluidized bed combustion, Naples, Italy, 2012, pp. 495–502.
- [49] W. Zhou, C. Zhao, L. Duan, X. Chen, D. Liu, A simulation study of coal combustion under O<sub>2</sub>/CO<sub>2</sub> and O<sub>2</sub>/N<sub>2</sub> atmospheres in circulating fluidized bed, *Chemical engineering journal* 223 (2013) 816–823.
- [50] W. Zhou, C. Zhao, L. Duan, X. Chen, C. Liang, Two-dimensional computational fluid dynamics simulation of nitrogen and sulfur oxides emissions in a circulating fluidized bed combustor, *Chemical engineering journal* 173 (2) (2011) 564–573.
- [51] W. Zhou, C. Zhao, L. Duan, D. Liu, X. Chen, Cfd modeling of oxy-coal combustion in circulating fluidized bed, *International Journal of Greenhouse Gas Control* 5 (6) (2011) 1489–1497.
- [52] W. Zhou, C. Zhao, L. Duan, D. Liu, X. Chen, Simulation study of oxy-fuel combustion in a circulating fluidized bed, in: The 35th International Technical Conference on Clean Coal & Fuel Systems, Clearwater, Florida, USA, 2010.
- [53] K. K. Win, W. Nowak, H. Matsuda, M. Hasatani, Z. Bis, J. Krzywanski, W. Gajewski, Transport velocity of coarse particles in multi-solid fluidized bed, *Journal of Chemical Engineering of Japan* 28 (5) (1995) 535–540.
- [54] J. Kotowicz, A. Balicki, Analysis of the thermodynamic and economic efficiency of supercritical power unit with cfb boiler fed with lignite and air separation unit based on high-temperature membrane technology, *Journal of Power Technologies* 93 (5) (2013) 308–313.
- [55] D. Pallares, F. Johnsson, Macroscopic modelling of fluid dynamics in large-scale circulating fluidized beds, *Progress in energy and combustion science* 32 (5) (2006) 539–569.
- [56] S. Kalogirou, Applications of artificial neural networks in energy systems, *Energy Conversion and Management* 40 (10) (1999) 1073–1087.
- [57] C. Zhao, L. Dun, W. Zhou, X. Chen, D. Zeng, T. Flynn, D. Kraft, Coal combustion characteristics on an oxy-cfb combustor with warm flue gas recycle, in: Proceedings of the 21st International Conference on Fluidized Bed Combustion, 2012, pp. 3–6.
- [58] R. R. Jensen, S. Karki, H. Salehfar, Artificial neural network-based estimation of mercury speciation in combustion flue gases, *Fuel Processing Technology* 85 (6) (2004) 451–462.
- [59] U. Kesgin, Genetic algorithm and artificial neural network for engine optimisation of efficiency and NO<sub>x</sub> emission, *Fuel* 83 (7) (2004) 885–895.
- [60] F. Christo, A. Masri, E. Nebot, T. Turanyi, Utilising artificial neural network and repro-modelling in turbulent combustion, in: Neural Networks, 1995. Proceedings., IEEE International Conference on, Vol. 2, IEEE, 1995, pp. 911–916.
- [61] S. Milanic, R. Karba, Neural network models for predictive control of a thermal plant, in: Proc. of the Int. Conf. EANN '96, London, UK, 1996, pp. 151–154.
- [62] B. Muller, H. Keller, Neural networks for combustion process modeling., in: Proc. of the Int. Conf. EANN '96, London, UK, 1996, pp. 87–90.
- [63] M. W. Gardner, S. Dorling, Artificial neural networks (the multilayer perceptron)—a review of applications in the atmospheric sciences, *Atmospheric environment* 32 (14) (1998) 2627–2636.
- [64] S. Arumugam, G. Sriram, P. S. Subramanian, Application of artificial intelligence to predict the performance and exhaust emissions of diesel engine using rapeseed oil methyl ester, *Procedia Engineering* 38 (2012) 853–860.
- [65] P. Boniecki, J. Dach, K. Pilarski, H. Piekarska-Boniecka, Artificial neural networks for modeling ammonia emissions released from sewage sludge composting, *Atmospheric Environment* 57 (2012) 49–54.
- [66] C. Carnevale, G. Finzi, E. Pisoni, M. Volta, Neuro-fuzzy and neural network systems for air quality control, *Atmospheric Environment* 43 (31)



- (2009) 4811–4821.
- [67] A. de Lucas, A. Durán, M. Carmona, M. Lapuerta, Modeling diesel particulate emissions with neural networks, *Fuel* 80 (4) (2001) 539–548.
- [68] Z. Hao, C. Kefa, M. Jianbo, Combining neural network and genetic algorithms to optimize low no<sub>x</sub> pulverized coal combustion, *Fuel* 80 (15) (2001) 2163–2169.
- [69] R. Karadağ, Ö. Akgöbek, The prediction of convective heat transfer in floor-heating systems by artificial neural networks, *International Communications in Heat and Mass Transfer* 35 (3) (2008) 312–325.
- [70] T. Kwater, Z. Kedzior, B. Twarog, Estimation by artificial neural network in ecological problems., in: *Proc. AMSE-Conference MS'2001, Lviv, Ukraine, 2001*, pp. 212–215.
- [71] J. Krzywanski, W. Muskała, W. Nowak, Application of neural networks for determining of the convective heat transfer coefficient in a circulating fluidized bed, *Power Engineering* 11 (2008) 761–764.
- [72] J. Krzywanski, W. Nowak, Modeling of heat transfer coefficient in the furnace of cfb boilers by artificial neural network approach, *International Journal of Heat and Mass Transfer* 55 (15) (2012) 4246–4253.
- [73] Y. Miyamoto, Y. Kurosaki, H. Fujiyama, E. Nanbu, Dynamic characteristic analysis and combustion control for a fluidized bed incinerator, *Control Engineering Practice* 6 (9) (1998) 1159–1168.
- [74] E. Molga, Neural network approach to support modelling of chemical reactors: problems, resolutions, criteria of application, *Chemical Engineering and Processing: Process Intensification* 42 (8) (2003) 675–695.
- [75] S. S. Nagendra, M. Khare, Artificial neural network approach for modelling nitrogen dioxide dispersion from vehicular exhaust emissions, *Ecological Modelling* 190 (1) (2006) 99–115.
- [76] L. E. Olcese, B. M. Toselli, A method to estimate emission rates from industrial stacks based on neural networks, *Chemosphere* 57 (7) (2004) 691–696.
- [77] S. L. Reich, D. Gomez, L. Dawidowski, Artificial neural network for the identification of unknown air pollution sources, *Atmospheric Environment* 33 (18) (1999) 3045–3052.
- [78] S. S. Sablani, A neural network approach for non-iterative calculation of heat transfer coefficient in fluid–particle systems, *Chemical Engineering and Processing: Process Intensification* 40 (4) (2001) 363–369.
- [79] Ü. A. Şahin, C. Bayat, O. N. Uçan, Application of cellular neural network (cnn) to the prediction of missing air pollutant data, *Atmospheric Research* 101 (1) (2011) 314–326.
- [80] S. Tasdemir, I. Saritas, M. Ciniviz, N. Allahverdi, Artificial neural network and fuzzy expert system comparison for prediction of performance and emission parameters on a gasoline engine, *Expert Systems with Applications* 38 (11) (2011) 13912–13923.
- [81] A. Tuma, H.-D. Haasis, O. Rentz, Development of emission orientated production control strategies using fuzzy expert systems, neural networks and neuro-fuzzy approaches, *Fuzzy sets and systems* 77 (3) (1996) 255–264.
- [82] Q. Wang, G. Xie, M. Zeng, L. Luo, Prediction of heat transfer rates for shell-and-tube heat exchangers by artificial neural networks approach, *Journal of Thermal Science* 15 (3) (2006) 257–262.
- [83] M. Xiaomin, Recognition of toxic gases emission in power plant based on artificial neural network, *Energy Procedia* 17 (2012) 1578–1584.
- [84] J. Zhang, F. Haghghat, Development of artificial neural network based heat convection algorithm for thermal simulation of large rectangular cross-sectional area earth-to-air heat exchangers, *Energy and Buildings* 42 (4) (2010) 435–440.
- [85] Y. Zhang, Y. Ding, Z. Wu, L. Kong, T. Chou, Modeling and coordinative optimization of no<sub>x</sub> emission and efficiency of utility boilers with neural network, *Korean Journal of Chemical Engineering* 24 (6) (2007) 1118–1123.
- [86] H. Zhou, K. Cen, J. Fan, Modeling and optimization of the no<sub>x</sub> emission characteristics of a tangentially fired boiler with artificial neural networks, *Energy* 29 (1) (2004) 167–183.
- [87] B. P. Grandjean, et al., Special issue on application of neural networks to multiphase reactors (2003).
- [88] C. Faur-Brasquet, P. Le Cloirec, Modelling of the flow behavior of activated carbon cloths using a neural network approach, *Chemical Engineering and Processing: Process Intensification* 42 (8) (2003) 645–652.
- [89] H. Lin, W. Chen, A. Tsutsumi, Long-term prediction of nonlinear hydrodynamics in bubble columns by using artificial neural networks, *Chemical Engineering and Processing: Process Intensification* 42 (8) (2003) 611–620.
- [90] A. Shaikh, M. Al-Dahhan, Development of an artificial neural network correlation for prediction of overall gas holdup in bubble column reactors, *Chemical Engineering and Processing: Process Intensification* 42 (8) (2003) 599–610.
- [91] G. Bollas, S. Papadokonstadakis, J. Michalopoulos, G. Arampatzis, A. Lappas, I. Vasalos, A. Lygeros, Using hybrid neural networks in scaling up an fcc model from a pilot plant to an industrial unit, *Chemical Engineering and Processing: Process Intensification* 42 (8) (2003) 697–713.
- [92] T. Abbas, M. Awais, F. Lockwood, An artificial intelligence treatment of devolatilization for pulverized coal and biomass in co-fired flames, *Combustion and flame* 132 (3) (2003) 305–318.
- [93] J. Kukkonen, L. Partanen, A. Karppinen, J. Ruuskanen, H. Junninen, M. Kolehmainen, H. Niska, S. Dorling, T. Chatterton, R. Foxall, et al., Extensive evaluation of neural network models for the prediction of NO<sub>2</sub> and PM<sub>10</sub> concentrations, compared with a deterministic modelling system and measurements in central Helsinki, *Atmospheric Environment* 37 (32) (2003) 4539–4550.
- [94] H. Ye, R. Nicolai, L. Reh, A bayesian–gaussian neural network and its applications in process engineering, *Chemical Engineering and Processing: Process Intensification* 37 (5) (1998) 439–449.
- [95] W. Muskała, J. Krzywański, T. Czakiert, W. Nowak, The research of CFB boiler operation for oxygen-enhanced dried lignite combustion, *Rynek Energii* 1 (92) (2011) 172–176.
- [96] J. Krzywański, R. Rajczyk, W. Nowak, Model research of gas emissions from lignite and biomass co-combustion in a large scale cfb boiler, *Chemical and Process Engineering* 35 (2) (2014) 217–231.

## Nomenclature

$\delta$	relative error,
$\lambda$	excess oxygen, -
A	ash content, wt.
C	carbon content, wt.
$C_{NO_x}$	nitrogen oxides concentration, ppm
Ca/S	calcium to sulfur molar ratio, -
CO <sub>2</sub>	oxygen concentration,
$d_{3,2}$	the Sauter diameter of coal particles
De	hydraulic furnace diameter, m
H	height of the combustion chamber, m
HSG	height of secondary gas inlet, m
mc	coal feed rate, kg·s <sup>-1</sup>
N	nitrogen content, wt.
$N_{iter}$	number of epochs, -
PG	primary gas ratio, -
R	flue gas recycle ratio,

- T average bed temperature, K  
v average gas velocity in the riser, m·s<sup>-1</sup>  
VM volatile matter content, wt.